Benzene/*tert*-Butyl Alcohol Interactions. 1. A Theoretical and Experimental Study

Gustavo Larsen,*,† Zohair K. Ismail,† Bruno Herreros,‡ and Rubén D. Parra‡

Department of Chemical Engineering, University of Nebraska–Lincoln, Nebraska 68588-0126, and Department of Chemistry, University of Nebraska–Lincoln, Nebraska 68588-0304

Received: February 11, 1998

The optimized structures of *tert*-butyl alcohol and *tert*-butyl alcohol/benzene (Tb–Tb and Tb–B) dimers were obtained by ab initio calculations at the HF/6-311++G(d,p) level, with electron correlation energy corrections using the local Møller–Plesset perturbation method. The small H-bond energies for these dimers are expected to be roughly overcome by the entropy change that accompanies the complexation reaction. Correlation times and temperature-dependent line width analysis of two selected benzene infrared bands in several liquid Tb–B mixtures indicate that there are marked mode-sensitive differences in the relaxation mechanisms taking place in solution. These are likely to be due to formation of Tb–B complexes similar to that predicted by gas-phase theoretical calculations.

Introduction

The study of weak hydrogen bonding systems has attracted renewed attention. In particular, the interaction of aromatic rings with weak- to medium-strength proton donors appears to play a role in the structure of certain biomolecules.[1] The study of thermodynamic and transport properties of binary and ternary mixtures involving alcohols and benzene is also an important field of research.[2–8] In the area of fossil fuels technology, oxygenate–hydrocarbon blends offer some key advantages over oxygenate-free formulations, such as increased octane numbers and reduced engine emissions.[9]

Alcohols possess the ability to form clusters (self-association) in the liquid phase via hydrogen bonding.[10–13] Theoretical calculations have been supportive of this idea.[14,15] Alcohol oligomers also form at the surface of solid acid catalysts, such as zeolite aluminosilicates.[16,17] On the other hand, less attention has been paid to the interaction of alcohols with aromatic molecules. To understand such interactions, previous studies dealing with simpler yet closely related systems, such as water–benzene and the ammonia–benzene (H_2O–B and NH_3–B), need to be taken into account. Using high-resolution optical and microwave spectroscopy in the gas phase, Rodham et al.[18] were able to show that the C_3 axis of rotation of the ammonia molecule is tilted by about 58° with respect to the C_6 axis of benzene, so that the hydrogen atoms in the former interact with the π electron cloud of the aromatic molecule. This is remarkable, considering that ammonia is a powerful proton acceptor, rather than a hydrogen donor. The dissociation of the H_2O–B complex has been obtained via an indirect method by Cheng and co-workers.[19] The difference between the ionization potential of B (monomer) and the appearance potential of the B^+ ion in the H_2O–B dimer gave a dissociation energy value for the complex of 2.25 ± 0.28 kcal/mol.[19] This value agrees well with results from ab initio calculations performed by Kim et al.[20] at the MP2/6-311++G(2d,p) and MP2/6-311++G(3df,2pd) levels, although these authors stress the fact that the energy difference between two different structures (one

of them being the absolute energy minimum geometry) was not significant. As expected, this type of π-H bonding becomes stronger with better hydrogen donors. Tang et al.[21] found that the stabilization energy of the B–HF complex predicted by ab initio calculations at the MP2/6-31G**/6-31G* level is −4.81 kcal/mol. It must be emphasized that this type of interaction is naturally extended to open-chain molecules (such as acetylene) with π electrons as well.[22]

From a fundamental standpoint, it appears interesting to study the nature of alcohol–benzene interactions since such pairs would contribute to the current understanding of hydrogen bonding with π electrons. This phenomenon may influence the thermodynamic and transport properties of alcohol–benzene solutions, providing that predictions derived from gas-phase theoretical calculations relate, at least qualitatively, to the behavior of such binary systems in the liquid phase.

The purpose of this contribution is to obtain the optimized theoretical structures of the *tert*-butyl alcohol–benzene (Tb–B) complex and *tert*-butanol dimer (Tb₂) by ab initio methods. Line shape analysis of two benzene Fourier transform infrared (FTIR) bands in Tb–B mixtures with different compositions suggests that intermolecular vibrational relaxation may be originated by the presence of a Tb–B complex in solution. In a future contribution, we plan to include self-consistent reaction field (SCRF) corrections to account for solvent effects. With regard to Tb₂, we must mention that trimers and tetramers of methanol have been predicted by theory,[14,15] but steric hindrance imposed by the methyl groups in the *tert*-butyl alcohol molecule may make the dimer the most important oligomeric form of this alcohol.

Methods

A. Computational Details. The Gaussian 94 program[23] was used for geometry optimizations and frequency calculations. Full geometry optimizations at the HF/6-311++G(d,p) level were performed on the individual molecules of benzene and *tert*-butyl alcohol and on the B–Tb and the Tb₂ complexes. Single-point energy calculations on the optimized structures were carried out using the Jaguar program.[24] The 6-311++G(d,p) basis set as implemented in the Jaguar program permits calculations with

* To whom all correspondence should be addressed.
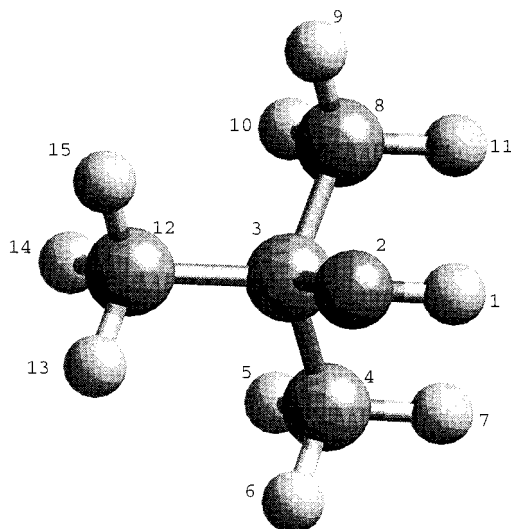† Department of Chemical Engineering.
‡ Department of Chemistry.

Benzene/*tert*-Butyl Alcohol Interactions. 1

J. Phys. Chem. A, Vol. 102, No. 24, 1998 **4735**

Figure 1. Optimized geometry of *tert*-butyl alcohol. Numbers are used to establish structural connections.

the pseudospectral method,[25–33] which is faster than the conventional analytical method. The electron correlation energy was corrected by the local Møller–Plesset perturbation method (LMP2).[34] This technique has been shown to result in superior accuracy for relative energy calculations compared to conventional MP2, due to elimination of basis set superposition error.[35] The basis set superposition error (BSSE) at the HF level was corrected by the counterpoise method.[36] The LMP2 method is already designed to avoid this error.

B. FTIR Measurements. The FTIR spectra of a number of binary Tb–B mixtures in the 400–4000 cm^{-1} range were measured with a computer-interfaced Nicolet 20SXB FTIR spectrometer at a spectral resolution of 4 cm^{-1}, using a variable-temperature liquid cell from Spectratech. Omnic software was used for data analysis. The solvents were dried for several days over molecular sieve 4A (Aldrich Chemical Co.). The mass fractions of the binary mixtures were determined by weight. The selected B FTIR bands were normalized and baseline-corrected. A computer program written in C language was used to carry out calculations involving correlation times.

Results and Discussion

A. Computational Results. *A.1. Optimized Structures.* The structures resulting from the geometry optimizations of the *tert*-butyl alcohol monomer and the B–Tb and Tb$_2$ complexes are shown in Figures 1–3. Additional information on the geometries is reported in Table 1. The r(C–C) and r(C–H) bond lengths in benzene were found to be 1.386 and 1.076 Å, respectively. Some relevant structural changes upon dimerization are presented in Table 2.

i. Benzene, tert-Butyl Alcohol, and B–Tb. The internal structure of each subunit is altered upon complexation. On one hand, the r(C–C) for the benzene molecule is increased by 0.001 Å and the r(C–H) remains unchanged. On the other hand, we observed a 0.001 Å increase in r(O–H) and a 0.0006 Å decrease in r(C–O) in the *tert*-butyl alcohol molecule. In the optimized structure of B–Tb, the distance from the center of the benzene ring to the H atom π-bonded to the ring is 3.27 Å. The corresponding X- -H–O angle, where X denotes the center of the ring, is 176.5°. The π-bonded H atom is tilted by 27.5° relative to the C$_6$ axis of benzene.

ii. tert-Butyl Alcohol and Tb$_2$. The optimized geometry of Tb$_2$ corresponds to a linear arrangement of the two subunits. In
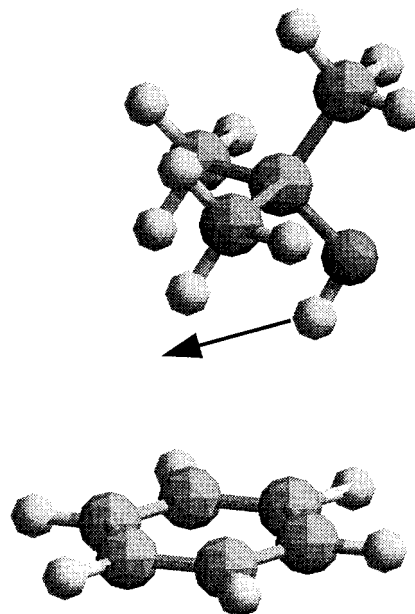

Figure 2. Optimized geometry of benzene-*tert*-butyl alcohol dimer (B–Tb). Relevant structural information is provided in Tables 1 and 2. The orientation of the total dipole moment is indicated by the arrow.
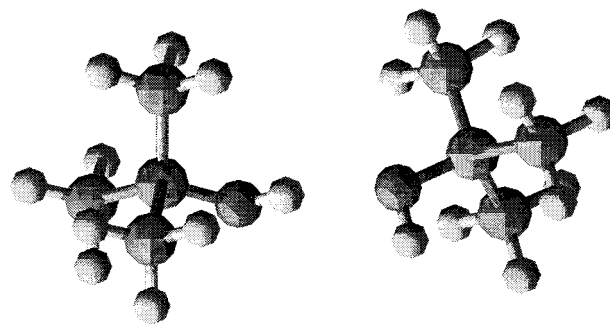

Figure 3. Optimized geometry of *tert*-butyl alcohol dimer (Tb$_2$). Relevant structural information is provided in Tables 1 and 2.

TABLE 1: Internal Coordinates of *tert*-Butyl Alcohol in the Monomer and in the B–Tb and Tb$_2$ Dimers (Distances in Å, Angles in deg). for Numbering, Refer to Figure 1

			Tb$_2$	
coordinates	monomer	B–Tb	donor	acceptor
R(O–H$_1$)	0.9410	0.9420	0.9455	0.9419
R(O–C$_3$)	1.4154	1.4148	1.4107	1.4246
R(C$_3$–C$_4$)	1.5299	1.5299	1.5308	1.5283
R(C$_3$–C$_1$)	1.5243	1.5245	1.5250	1.5240
R(C$_3$–C$_8$)	1.5299	1.5299	1.5310	1.5286
R(C$_4$–H$_{17}$)	1.0860	1.0864	1.0867	1.0858
R(C$_4$–H$_{18}$)	1.0851	1.0853	1.0855	1.0880
R(C$_4$–H$_{19}$)	1.0881	1.0875	1.0870	1.0850
R(C$_{12}$–H$_{26}$)	1.0860	1.0862	1.0864	1.0846
R(C$_{12}$–H$_{25}$)	1.0849	1.0850	1.0852	1.0857
R(C$_{12}$–H$_{15}$)	1.0849	1.0850	1.0852	1.0857
θ(C$_3$–O–H$_{13}$)	110.12	110.23	110.63	109.96
θ(C$_4$–C$_3$–O)	109.52	109.55	109.66	109.07
θ(C$_8$–C$_3$–O)	109.52	109.55	109.70	109.20
θ(C$_{12}$–C$_3$–O)	105.30	105.40	105.65	105.48

this structure one subunit acts as a H-donor and the other as an acceptor. The r(O–H) is lengthened by 0.0045 Å in the donor and by 0.0009 Å in the acceptor, with respect to the free Tb. The r(C–O) is shortened by 0.0047 Å in the donor and increased by 0.0106 Å in the acceptor relative to the free monomer. The r(O- - -H) and r(O- - -O) are calculated to be 2.076 and 3.014 Å, respectively.

TABLE 2: Some Relevant Geometric Aspects of the B–Tb and Tb₂ Dimers (Distances in Å, Angles in deg). "X" Denotes the Center of the Benzene Ring; "C₆" Denotes the C_6 Axis of Benzene

				B–Tb			
$\Delta R(C-C)$	$\Delta R(O-H)$	$\Delta R(C-O)$	$\Delta\theta(C-O-H)$	$R(X--H)$	$R(X--O)$	$\theta(X-H-O)$	$\theta(H--C_6--X)$
0.001	0.0011	−0.0006	0.1056	3.2734	4.2141	176.50	27.50

	Tb₂		
	$\Delta R(O-H)$	$\Delta R(C-O)$	$\Delta\theta(C-O-H)$
donor	0.0045	−0.0047	0.492
acceptor	0.0009	0.0106	−0.166

		Tb₂ (Donor–Acceptor)		
$R(O-O)$	$R(O-H)$	$\theta(O-H-O)$	$\theta(H-O--H)$	$\tau(H-O--H-O)$
3.0136	2.076	171.05	110.50	−72.60

TABLE 3: Electronic Interaction Energies Given by the Analytic and the Pseudospectral Methods

		B–Tb	
		pseudospectral	
	analytic HF	HF	LMP2
case 1	−1.541	−1.110	−3.853
case 2	−1.546	−1.126	−3.479
case 3	−1.181	−0.973	−3.326

		Tb₂	
		pseudospectral	
	analytic HF	HF	LMP2
case 1	−4.463	−4.300	−5.164
case 2	−4.549	−4.371	−5.048
case 3	−3.978	−3.931	−4.608

A.2. Electronic Interaction Energies. The electronic portion of the interaction energies of B–Tb and Tb₂ dimers with and without counterpoise corrections for basis set superposition error (BSSE) is summarized in Table 3. Two different methods were used to calculate the interaction energies, namely the analytical method as implemented in the Gaussian 94 program and the pseudospectral method as set up in the Jaguar program. The former was used to calculate energies at the HF level, while the latter was run at both HF and LMP2 levels. The 6-311++G-(d,p) basis set was used throughout. The electronic interaction energies for B–Tb were calculated from the equation

$$\Delta E = E(B-Tb) - \{E(B)_a - E(Tb)_a\}$$

with the same approach used for Tb₂. In this equation the subscript *a* indicates whether the energy of the subunit is calculated using the optimized geometry of an isolated molecule (case 1) or the geometry that it has in the optimized dimer (case 2). In general, we see that at the HF level the analytical method gives larger binding energies. However, after BSSE correction both methods give similar results, especially for the Tb₂ complex. As expected, correlation adds to the H-bond energies in both B–Tb and Tb₂. This effect is significantly larger for the weaker π-bonded B–Tb system, where it accounts for more than twice the entire SCF interaction energy itself. It is interesting to note that the energy cost for deformation of each subunit upon complexation is more pronounced after correlation correction. For instance, at the LMP2 level the interaction energy for B–Tb is −3.85 kcal/mol in case 1 and −3.48 kcal/mol in case 2, which gives a deformation energy cost of about 0.37 kcal/mol. At the HF level this energy cost is about 0.001 kcal/mol.

A.3. Vibrational Frequencies. The fully optimized geometries of the monomers and dimers were used to calculate the normal-mode frequencies and theoretical infrared intensities using the harmonic approximation. The results are listed in Table 4. Several comments are in order.

i. tert-Butyl Alcohol and tert-Butyl Alcohol Dimer (Tb₂). Upon complexation there is a sizable red shift (78 cm⁻¹) in the stretching mode of the donor O–H bond. The intensity is significantly increased (∼10 times), which reflects the perturbation induced on this mode by the formation of the H-bond. The frequency and intensity of the O–H stretching mode of the acceptor molecule are not changed much in comparison to the monomer. Another important mode is the C–O stretch. It is seen that the C–O acceptor band is red-shifted about 13 cm⁻¹, while the donor C–O stretching frequency is shifted to the blue by 6 cm⁻¹.

Dimerization also influences the O–H torsional and O–H bending modes. Both torsional modes are blue-shifted significantly. The acceptor O–H torsional frequency is shifted by 22 cm⁻¹, and the donor by 341 cm⁻¹. We found that the normal modes of the monomer at 1251 and 1464 cm⁻¹ are composed of basically a mixture of O–H bending and CH₃ wag-type vibrations. These bands are displaced to higher frequencies, with the shift for the donor being about 4 times that of the acceptor.

ii. tert-Butyl Alcohol and Benzene-tert-Butyl Alcohol (B–Tb). The same qualitative trends seen upon Tb₂ dimerization are also noted upon B–Tb dimerization. In the B–Tb dimer, the *tert*-butyl alcohol molecule acts as a H-donor, and therefore the calculated frequency and intensity changes are similar (though smaller) to those found for the donor moiety in the Tb₂ complex. The vibrational frequencies and intensities of benzene are largely unaffected by complexation, which is consistent with the small structural changes mentioned above.

A.4. Thermodynamic Quantities. To estimate some thermodynamic parameters, we have used the calculated vibrational modes and standard formulas.[37] To account for anharmonicity and correlation effects, the calculated frequencies are scaled by a factor of 0.89. The results are shown in Tables 5 and 6.

The full thermodynamic interaction energy is given by

$$\Delta E = \Delta E_{\text{elec}} + \Delta E_{\text{ZPVE}} + \Delta E_{\text{vib,therm}} + \Delta E_{\text{trans}} + \Delta E_{\text{rot}}$$

where each term on the right corresponds to the difference between the product (dimer) and reactants (subunits).

The correlated electronic contributions to the interaction energies of the Tb₂ and B–Tb dimers are −4.61 and −3.33 kcal/mol, respectively. These values are lessened as a result of the greater zero-point vibrational energy (E_{ZPVE}) and thermal vibrational energy ($E_{\text{vib,therm}}$) in the dimers relative to the monomers. Translation and rotation each adds 0.90 kcal/mol to the binding energy. The estimated value of ΔE at 298.15 K

TABLE 4: Frequencies (cm^{-1}) and Intensities (kcal/mol) of *tert*-Butyl Alcohol and Benzene, and Changes Resulting from Formation of the B−Tb and Tb$_2$ Complexes. In Bold, We Denote Those Vibrational Modes That Are Discussed in Some Detail

type	Tb ν	Tb I	Tb (donor) Δν	Tb (donor) ΔI	Tb (acceptor) Δν	Tb (acceptor) ΔI	B−Tb Δν	B−Tb ΔI	B ν	B I	B−Tb Δν	B−Tb ΔI
	221	3	2	−2	4	−3	1	−3	448	0	0	0
	281	27	8	−25	7	−23	6	−26	448	0	1	0
	295	0	1	0	0	0	0	0	662	0	−1	0
OH torsion	**311**	**97**	**341**	**−96**	**22**	**19**	70	−89	662	0	−1	0
	363	1	1	1	1	5	−3	1	755	149	3	19
	365	9	1	−9	8	9	−1	61	769	0	−8	0
	447	0	0	6	2	1	0	0	954	0	1	0
	494	11	6	−4	−2	−9	3	0	954	0	2	1
	501	12	9	102	0	1	0	0	1070	0	−2	0
	795	3	1	−1	−2	42	0	−1	1090	0	0	0
	983	0	−2	0	4	0	0	0	1099	0	−1	0
	995	0	−1	0	3	0	0	0	1099	0	−1	0
CO stretch	**1028**	**40**	**6**	**−40**	**−13**	**20**	2	−1	1118	0	−4	0
	1035	0	1	36	4	0	1	0	1128	5	−1	−1
	1114	18	8	−1	4	−7	2	−2	1128	5	−1	0
	1133	2	0	1	2	0	1	1	1180	0	−1	0
OH bend.	**1251**	**54**	**40**	**31**	**10**	**−10**	9	0	1280	0	−1	0
	1360	74	1	−48	−10	40	1	5	1280	0	0	0
	1364	23	1	29	5	−7	0	−6	1338	0	0	0
OH bend.	**1465**	**39**	**26**	**8**	**6**	**−13**	5	−11	1491	0	0	0
	1526	16	−2	0	4	6	0	−1	1629	10	−1	1
	1535	26	0	1	3	6	−1	−6	1629	10	−1	1
	1552	5	−2	−2	4	0	−1	1	1774	0	−3	0
	1590	0	0	0	2	0	0	0	1774	0	−3	0
	1601	0	0	0	0	0	0	0	3311	0	2	0
	1603	0	1	0	3	0	1	0	3322	0	2	0
	1615	2	0	0	2	0	0	0	3322	0	3	0
	1623	4	2	0	1	1	0	−1	3341	45	1	−12
	1634	7	2	−5	0	7	1	−1	3341	45	1	−10
	3150	21	2	−4	2	5	3	0	3352	0	1	0
	3157	51	0	−14	2	−2	1	−12				
	3171	7	−2	6	2	−1	−1	−14				
	3208	6	2	−3	3	−1	2	−2				
	3218	81	1	−7	2	−13	1	7				
	3231	6	−6	−10	2	−2	−3	6				
	3232	6	−7	14	6	13	−3	2				
	3242	59	−7	37	2	9	−4	−2				
	3243	59	−5	−1	5	−3	−2	−2				
OH stretch	**4171**	**37**	**−78**	**295**	**−9**	**5**	−14	75				

TABLE 5: Properties of *tert*-Butyl Alcohol and Benzene Monomers, and Tb$_2$ and B−Tb Dimers at 298 K and 1 atm (Energies in kcal/mol, S in cal/mol K)

	benzene		B−Tb	
$E_{vib,therm.}$	0.794	1.40	5.933	8.12
$S_{trans.}$	38.54	39.38	40.54	41.37
$S_{rot.}$	25.35	25.86	30.88	31.38
$S_{vib.}$	3.86	5.89	54.77	62.09

	tert-butyl alcohol		Tb$_2$	
$E_{vib,therm.}$	2.113	3.102	6.945	9.475
$S_{trans.}$	38.39	39.22	40.46	41.29
$S_{rot.}$	25.30	25.80	30.62	31.12
$S_{vib.}$	11.93	15.25	55.81	64.30

B−Tb at 273.15 K

$\Delta E_{vib.}$	ΔS_T	$\Delta S_{rot.}$	ΔS_V	ΔS	ΔE	ΔH	ΔG
3.026	−36.4	−19.77	38.97	−17.20	−1.79	−2.389	2.318

Tb−Tb at 273.15 K

$\Delta E_{vib.}$	ΔS_T	$\Delta S_{rot.}$	ΔS_V	ΔS	ΔE	ΔH	ΔG
2.719	−36.3	−19.98	31.96	−24.35	−2.75	−3.335	3.315

is then −1.50 and −2.47 kcal/mol for B−Tb and Tb$_2$, respectively. The enthalpy of binding energy is more negative by room temperature. When combined with the negative value of ΔS, the Gibbs free energy of dimerization is positive in each case, with that of Tb$_2$ being larger. Hence, the small H-bond energies for these dimers are expected to be overcome by the loss of entropy that accompanies the complexation process. However, the 0.89 correction factor is known to be a rather

crude correction for anharmonic effects. Therefore, unless anharmonic corrections are made more rigorous, any analysis must be done with caution.

A.5. Dipole Moment Enhancement. The change in dipole moment upon dimerization is obtained as the difference between the dipole moment of the corresponding cluster (Tb$_2$, B−Tb) and that obtained by vectorial addition of the individual dipole moments. To calculate the dipole moment of each subunit, the

TABLE 6: Thermodynamic Parameters of B–Tb and Tb$_2$ Dimerization (ΔE, ΔH, and ΔG in kcal/mol, ΔS in cal/mol K)

	B–Tb	Tb$_2$
$\Delta E_{elect.}$	−3.326	−4.608
ΔE_{ZPVE}	0.289	0.922
ΔE	−1.495	−2.470
ΔH	−2.085	−3.060
ΔS	−16.86	−24.08
ΔG	3.53	4.12

TABLE 7: Dipole Moment of Benzene and *tert*-Butyl Alcohol, and Enhanced Dipole Moment upon Dimerization (Debye Units)

	μ	$\Delta\mu$
benzene	0.0093	
tert-butyl alcohol	1.7543	0.0769
B–Tb	1.8404	
tert-butyl alcohol (donor)	1.7691	
tert-butyl alcohol (acceptor)	1.7358	0.6179
Tb$_2$	2.6799	

complete set of basis functions of the dimers was used and the geometry of each monomer was frozen in that of the optimized dimer. The results are listed in Table 7. It is clear that formation of the H-bond leads to an enhancement of the dipole moment relative to the two free subunits, although this effect is more pronounced in the Tb$_2$ dimer.

B. Analysis of FTIR Data. A key question that remains is whether an interaction similar to that inferred by gas-phase theoretical calculations is present in the liquid state. A detailed description of the B–Tb interactions would require good knowledge of a number of macroscopic properties. For example, the dielectric constant is expected to be a strong function of composition. This, in turn, is expected to affect the structure of associated species. It is clear that conventional frequency shifts in benzene are not expected (see section A.4). Similarly, a simple analysis of *tert*-butyl alcohol bands in the liquid mixture will be complicated by a number of factors, including the difficulties associated by uncoupling alcohol–alcohol and alcohol–benzene contributions. One way to gain some insight into the possible molecular orientations in liquids is through the study of relaxation phenomena. Spectroscopic techniques such as NMR and FTIR can be used to derive, by means of line shape analysis, the molecular motions and intermolecular correlations in the liquid state.[38,39] In particular, it has been stressed that this type of infrared band analysis is complicated by the fact that it is difficult to uncouple vibrational relaxation mechanisms from those involving rotational motion in the liquid medium.[39] It must be recognized that, in general, linewith analysis of conventional spectroscopies yields the convoluted dephasing rates of more than one contribution.[40] This is the reason ultrafast infrared spectroscopy is favored over conventional FTIR, given the fact that the former allows for direct time-resolved measurements.[41] Nevertheless, it is possible to infer qualitatively which modes in the benzene molecule are more likely to be affected by intermolecular vibrational relaxation. For relatively large polyatomic molecules such as benzene, internal vibrational relaxation can occur quickly among the many modes before energy is transferred to the condensed medium via intermolecular mechanisms. For example, it has been reported that the C–H stretch in benzene relaxes in about 1 ps.[42] However, it has long been recognized that *hydrogen bonding* and *dipole–dipole* interactions indeed facilitate markedly the intermolecular energy transfer.[43] This is due to the
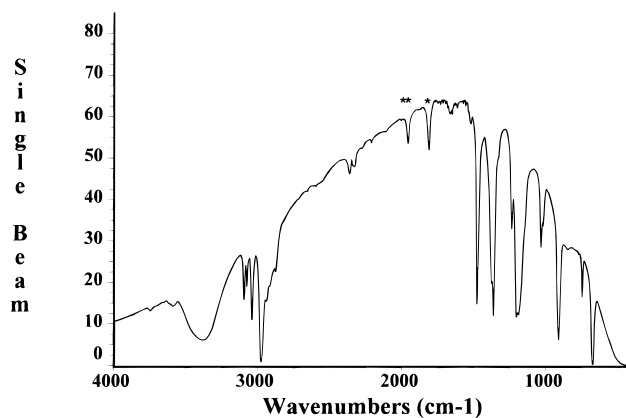
Figure 4. Spectrum of 50:50 benzene–*tert*-butyl alcohol binary mixture.
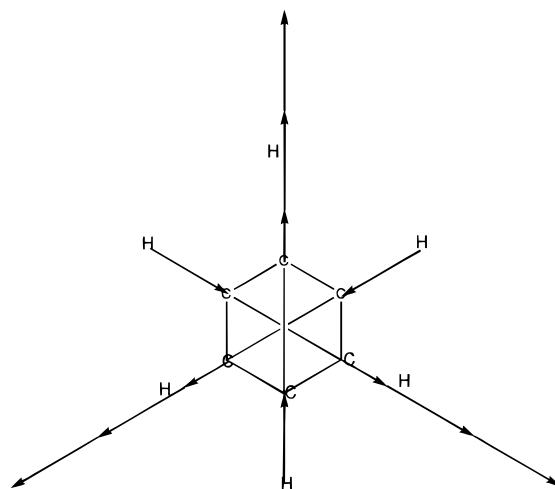
Figure 5. In-plane benzene C–H stretching mode. The double-starred peak in Figure 4 is the first overtone of this mode.
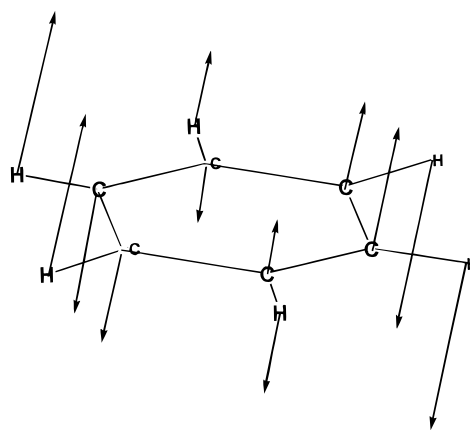
Figure 6. Out-of-plane benzene C–H stretching mode. The starred peak is the first overtone of this mode.

fact that hydrogen bonding creates an additional relaxation channel by simple intermolecular bond breaking.[44] The FTIR spectrum of a 50:50 Tb–B mixture is shown in Figure 4. Our selection of a specific pair of benzene vibrational modes for line shape analysis was not arbitrary. Note that, in one case, in-plane C–H stretching takes place (mode 1, Figure 5), whereas the remaining mode (mode 2, Figure 6) is due to out-of-plane C–H bending. An important observation is that their oscillating dipole moments are perpendicular; that is, the vibrationally excited benzene molecule is intuitively expected to behave
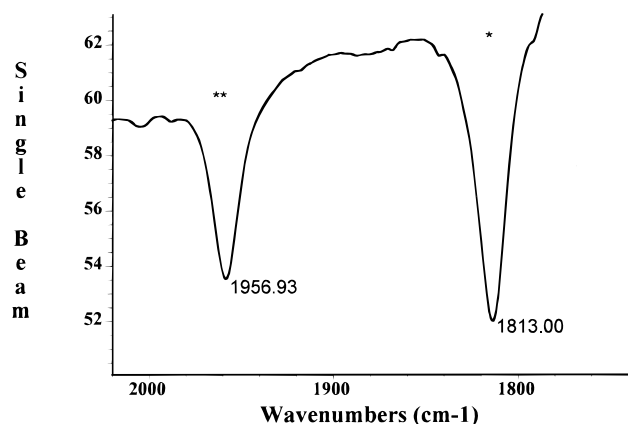
Figure 7. Starred and double-starred FTIR peaks in an expanded scale.

Figure 8. Correlation function analysis for the 50:50 binary mixture: (●) mode in Figure 6, (□) mode in Figure 5.

differently in each case with regard to relaxation in the Tb−B complex, providing dipole−dipole relaxation plays an important role.

Small alcohols such as methanol are expected to form open oligomeric chains at high concentrations in benzene solutions, as predicted by Monte Carlo simulations.[45] Using resonant ion-dip infrared spectroscopy, Pribble et al.[46] were able to observe methanol$_n$−benzene clusters ($n = 1-6$) and modeled the minimum energy structures of the complexes with $n = 1$ and 2 with density functional theory (DFT) at the Becke3LYP/6-31+G* level. Interestingly, the predicted spatial orientation of their $n = 1$ structure is very similar to our Tb−B model, and the second alcohol molecule in the $n = 2$ complex hydrogen-bonds to the first methanol molecule (the latter essentially oriented as in the $n = 1$ case with respect to the benzene molecule) away from the C_6 axis of benzene. Earlier, we mentioned that we do not expect Tb to yield oligomers with $n = 3$ and above due to steric limitations. Thus, the interaction of benzene and *tert*-butyl alcohol in the liquid phase may well be limited to the Tb−B and Tb$_2$−B case, both of them having similar orientations with respect to the center of the ring and the main O−H interacting group.

We proceeded to compare the correlation times of these two different vibrational modes of benzene to explore whether there is preferential orientation for energy (vibrational) relaxation, which in turn can be ascribed to a local B−Tb interaction. Their expanded spectrum is shown in Figure 7. The starred and double-starred peaks represent the first overtones of the vibrational modes in benzene depicted in Figures 5 and 6, as determined by Gaussian 94.

Studying benzene/toluene mixtures, Reimschüssel and Abramczyk[39] were able to determine which lines are affected by vibrational relaxation effects. The idea is to calculate the correlation functions for a few such bands. When one or more of these functions (each one associated with one particular IR band) are found to deviate from the general trend, it then becomes apparent that such anomalies must be ascribed to departure from purely rotational relaxation phenomena. An interesting observation is that apparently dissimilar vibrational modes will have very similar correlation functions if other phenomena such as vibrational relaxation do not play a role. Since the correlation function is in principle a measure of the probability of finding the molecule in its excited vibrational state as a function of time, a more rapidly decaying correlation function in a specific vibrational mode can be associated with a preference of the molecule to selectively relax its vibrational energy along a specific path.
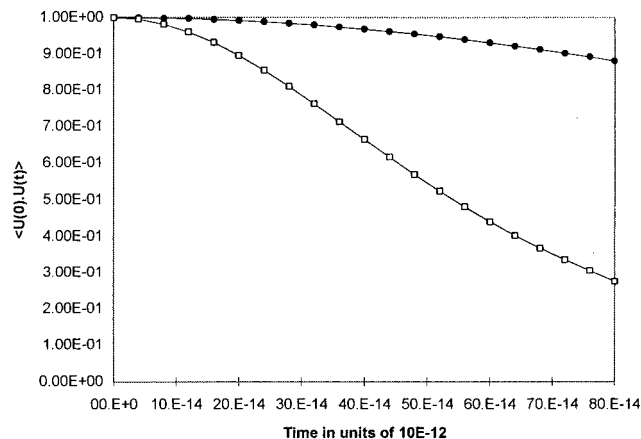
The following formulas for line shape analysis were used:[38,39]

$$\text{Zeroth moment } (\eta_0) = \sum_{\omega=\omega_0}^{\omega_1} I(\omega) \approx \int I(\omega)\, d\omega$$

$$\text{First moment } (\eta_1) = \sum_{\omega=\omega_0}^{\omega_1} \omega I(\omega) \approx \int \omega I(\omega)\, d\omega$$

where I represents the intensity. Evaluation of the band center, ω_0, is obtained from the zeroth moment (area) and first moments (center of mass) of the band,

$$\omega_0 \approx \int I(\omega)\omega\, d\omega / \int I(\omega)\, d\omega$$

From the band center (ω_0) evaluation, we may infer the difference between any frequency and that of the band center (frequency displacement). The initial-state-averaged transition probability is represented by

$$I(\omega) = \frac{\sigma(\omega)}{\omega[1 - \exp(-\hbar\omega/kT)]}$$

where $\sigma(\omega)$ represents the value of the ordinate in terms of the complement (100-transmission), i.e., the absorption coefficient in terms of the band center (ω_0) and the observed (angular) frequency of the vibrational transition of the isolated molecule. The above equation could also be explained as the ratio of the initial-state-averaged transition probability to the zeroth moment.

The dipole correlation function $\langle u(0)\, u(t)\rangle$, in terms of the normalized spectral intensity ($\lambda(\omega) = I(\omega)/\eta_0$), is

$$\int \lambda(\omega) \cos[(\omega - \omega_0)t]\, dt$$

The quantity $u(t)$ in the correlation time function is a unit vector at time (t) along the direction of the permanent dipole moment of a molecule.

$$\tau_c = \int_0^\infty \langle u(0)\, u(t)\rangle\, dt$$

where τ_c is the rotational correlation time, which, if unaffected by vibrational relaxation mechanisms, should be very similar for the two benzene C−H modes under study.

For the 50:50 mixture, we carried out the correlation function analysis described above and obtained the curves shown in Figure 8. It is immediately apparent that the benzene vibrational
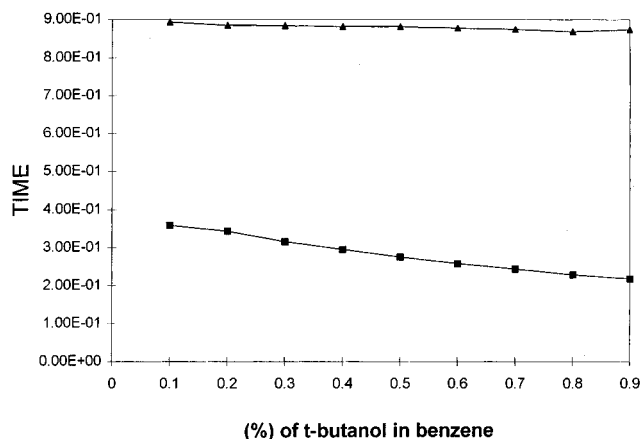
Figure 9. Value of correlation function at a fixed correlation time for different B−Tb compositions: (▲) mode in Figure 6, (■) mode in Figure 7.
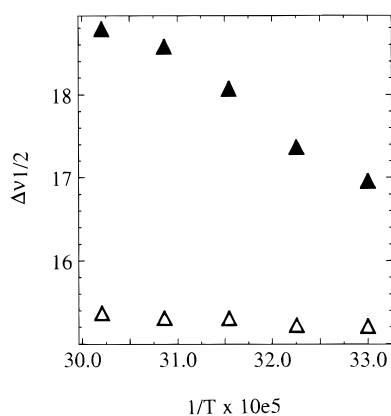

Figure 10. $\Delta\nu_{1/2}$ vs T plots for the 70% Tb−B mixture: (△) mode in Figure 5, (▲) mode in Figure 6.

mode that generates an oscillating dipole with an orientation closer to the permanent dipole moment of the Tb−B adduct predicted by theory (see Figures 2, 5, and 6) relaxes much faster than the one that produces an out-of-plane oscillating dipole moment. Before taking this observation as an indication of intermolecular dipole−dipole relaxation, it is necessary to demonstrate that the former is much less sensitive to concentration changes, i.e., that it is less influenced by the presence of the other species (*tert*-butyl alcohol). In Figure 9, we show the value of the correlation function at a fixed correlation time for different B−Tb compositions. Again, it is seen that adding more alcohol decreases the correlation function much more rapidly for the mode shown in Figure 5. Such strong dependence with composition calls for intermolecular relaxation in the latter.

It is also interesting to study the temperature dependence of the IR full width at half-maximum for the same two vibrational modes. In the Rakov's method,[47] a Lorentzian profile is assumed, which results in additive rotational and vibrational widths,

$$\Delta\nu_{1/2} = \delta + A \exp(-U/kT)$$

where U is the potential barrier to rotation, and δ is the vibrational contribution. As expected for small temperature changes, the latter is safely assumed to remain constant. Figure 10 shows that the $\Delta\nu_{1/2}$ of the in-plane C−H mode of benzene is not a function of temperature (i.e., it is dominated by vibrational relaxation) at high alcohol concentrations, but the

C−H bending mode has an important temperature dependence. Interestingly, we have observed that the $\Delta\nu_{1/2}$ of both modes is affected by temperature in pure benzene and at low alcohol concentrations (not shown), which also supports the idea that preferential Tb−B orientations induce intermolecular Tb → B vibrational relaxation phenomena in Tb-rich solutions. We have not attempted to fit the data for the C−H bending mode shown in Figure 10 to the Rakov's three-parameter (δ, A, $-U/k$) equation because of the small experimental error in $\Delta\nu_{1/2}$ and the limited number of data points. However, it is qualitatively clear that the exponential (rotational) temperature dependence in the in-plane C−H mode of benzene is virtually nonexistent.

Unfortunately, a similar analysis could not be done on *tert*-butyl alcohol bands because (i) they invariably overlapped with benzene signals and (ii) they are expected to be affected by alcohol−alcohol interactions as well. Nevertheless, our line shape analysis suggests that intermolecular vibrational relaxation is likely to occur via formation of weak Tb−B complexes similar to those predicted by gas-phase calculations. In a future contribution, we plan to extend our theoretical studies on Tb−B and Tb$_2$ complexes to include the use of self-consistent reaction field corrections in an effort to simulate solvent effects.

References and Notes

(1) (a) Burley, S. K.; Petsko, G. A. *FEBS Lett.* **1986**, *203*, 139. (b) Scheiner, S. *Hydrogen Bonding: A Theoretical Perspective*; Oxford University Press: New York, 1997.

(2) Wormald, C. J.; Sowden, C. J. *J. Chem. Thermodyn.* **1997**, *29*, 1223.

(3) Kouris, S.; Panayiotou, C. *J. Chem. Eng. Data* **1989**, *34*, 200.

(4) Skomorokhov, V. I.; Borisov, V. B. *Russ. J. Appl. Chem.* **1993**, *66*, 962.

(5) Ramprasad, G.; Mukherjee, A. K.; Das, T. R. *J. Chem. Eng. Data* **1991**, *36*, 124.

(6) Bhardwaj, U.; Maken, S.; Singh, K. C. *J. Chem. Thermodyn.* **1996**, *28*, 1173.

(7) Rodriguez, V.; Lafuente, C.; Lopez, M., *J. Chem. Thermodyn.* **1993**, *25*, 679.

(8) Kurihara, K.; Uchiyama, M.; Kojima, K. *J. Chem. Eng. Data* **1997**, *42*, 149.

(9) Rice, R. W.; Sanyal, A. K.; Elrod, A. C. *Trans. ASME J. Eng.* **1991**, *113*, 377.

(10) Dixon, J. R.; George, W. O.; Price, J. M. *J. Chem. Soc., Faraday Trans.* **1997**, *93*, 3611.

(11) Schwager, F.; Marand, E.; Davis, R. M. *J. Phys. Chem.* **1996**, *100*, 19268.

(12) Buck, U.; Siebers, J.-G.; Wheatley, R. J. *J. Chem. Phys.* **1998**, *108*, 20.

(13) Brot, C. *Z. Phys. D* **1989**, *11*, 249.

(14) (a) Mo, O.; Yañez, M.; Elguero, J., *J. Mol. Struct.* **1994**, *314*, 73. (b) Mo, O.; Yañez, M.; Elguero, J. *J. Chem. Phys.* **1997**, *107*, 3592.

(15) MacLean, E. J.; Harris, K. D. M.; Price, S. L. *Chem. Phys. Lett.* **1994**, *225*, 273.

(16) Haase, F.; Sauer, J. *J. Am. Chem. Soc.* **1995**, *117*, 3780.

(17) Mirth, G.; Lercher, J. A.; Anderson, M. W.; Klinowsky, J. *J. Chem. Soc., Faraday Trans.* **1990**, *86*, 3039.

(18) (a) Rodham, D. A.; Suzuki, S.; Suenram, R. D.; Lovas, F. J.; Dasgupta, S.; Goddard, W. A., III; Blake, G. A. *Nature* **1993**, *362*, 735. (b) Fredericks, S. Y.; Pedulla, J. M.; Jordan, K. D.; Zwier, T. S. *Theor. Chem. Acc.* **1997**, *96*, 51.

(19) Cheng, B.-M.; Grover, J. R.; Walters, E. A. *Chem. Phys. Lett.* **1995**, *232*, 364.

(20) Kim, K. S.; Lee, J. Y.; Choi, H. S.; Kim, J.; Jang, J. H. *Chem. Phys. Lett.* **1997**, *265*, 497.

(21) Tang, T.-H.; Hu, W.-J.; Yan, D.-Y, *J. Mol. Struct.* **1990**, *207*, 319, b) Rozas, I.; Alkorta, I.; Elguero, J. *J. Phys. Chem. A* **1997**, *101*, 9457.

(22) Tang, T.-H.; Cui, Y.-P. *Can. J. Chem.* **1996**, *74*, 1162.

(23) Frisch, M. J.; Trucks, G. W.; Schlegel, H. B.; Gill, P. M. W.; Johnson, B. G.; Robb, M. A.; Cheeseman, J. R.; Keith, T.; Petersson, G. A.; Montgomery, J. A.; Raghavachari, K.; Al-Laham, M. A.; Zakrzewski, V. G.; Ortiz, J. V.; Foresman, J. B.; Cioslowski, J.; Stefanov, B. B.; Nanayakkara, A.; Challacombe, M.; Peng, C. Y.; Ayala, P. Y.; Chen, W.; Wong, M. W.; Andres, J. L.; Repogle, E. S.; Gomperts, R.; Martin, R. L.; Fox, D. J.; Binkley, J. S.; Defrees, D. J.; Baker, J.; Stewart, J. P.; Head-Gordon, M.; Gonzalez, C.; Pople, J. A. *Gaussian 94*; Gaussian Inc.: Pittsburgh, PA, 1995.

(24) Friesner, R. A. *Chem. Phys. Lett.* **1985**, *116*, 39.

(25) Friesner, R. A. *J. Chem. Phys.* **1986**, *85*, 1462.

(26) Friesner, R. A. *J. Chem. Phys.* **1987**, *86*, 3522.

(27) Friesner, R. A. *J. Phys. Chem.* **1988**, *92*, 3091.

(28) Ringnalda, M. N.; Won, Y.; Friesner, R. A. *J. Chem. Phys.* **1990**, *92*, 1163.

(29) Langlois, J.-M.; Muller, R. P.; Coley, T. R.; Goddard, W. A., III; Ringnalda, M. N.; Won, Y.; Friesner, R. A. *J. Chem. Phys.* **1990**, *92*, 7488.

(30) Ringnalda, M. N.; Belhadj, M.; Friesner, R. A. *J. Chem. Phys.* **1990**, *93*, 3397.

(31) Won, Y.; Lee, J.-G.; Ringnalda, M. N.; Friesner, R. A. *J. Chem. Phys.* **1991**, *94*, 8152.

(32) Friesner, R. A. *Annu. Rev. Phys. Chem.* **1991**, *42*, 341.

(33) Pollard, W. T.; Friesner, R. A. *J. Chem. Phys.* **1993**, *99*, 6742.

(34) Saebo, S.; Pulay, P. *Annu. Rev. Phys. Chem.* **1993**, *44*, 213.

(35) Saebo, S.; Pulay, P. *J. Chem. Phys.* **1993**, *98*, 2170.

(36) Boys, S. F.; Bernardi, F. *Mol. Phys.* **1970**, *19*, 553.

(37) Hill, T. L. *An Introduction to Statistical Thermodynamics*; Addison-Wesley: Reading, MA, 1960; p 167.

(38) Rothschild, W. G. *Macromolecules* **1968**, *1*, 43.

(39) Reimschussel, W.; Abramczyk, H. *Chem. Phys. Lett.* **1980**, *73*, 565.

(40) Owrutsky, J. C.; Raftery, D.; Hochstrasser, R. M. *Annu. Rev. Phys. Chem.* **1994**, *45*, 519.

(41) Hong, X.; Chen, S.; Dlott, D. D. *J. Phys. Chem.* **1995**, *99*, 9102.

(42) Fendt, A.; Fischer, S. F.; Kaiser, W. *Chem. Phys.* **1981**, *57*, 55.

(43) Shin, H. K. *Chem. Phys. Lett.* **1974**, *26*, 450.

(44) Graener, H.; Ye, T. Q.; Laubereau, A. *J. Chem. Phys.* **1989**, *90*, 3413.

(45) Adachi, Y.; Nakanishi, K. *Fluid Phase Equilib.* **1993**, *83*, 69.

(46) Pribble, R. N.; Hagemeister, F. C.; Zwier, T. S. *J. Chem. Phys.* **1997**, *106*, 2145.

(47) Vincent-Geisse, J.; Soussen-Jacob, J. In *Organic Liquids: Structure, Dynamics and Chemical Properties*; Buckingham, A. D., et al., Eds.; J. Wiley and Sons, Chichester, 1978.